[PROC. OF JSCE No. 344/ I -1 (Structural Eng. /Earthquake Eng.) April 1984]

A TOTAL LAGRANGIAN NONLINEAR ANALYSIS OF ELASTIC TRUSSES

By Fumio NISHINO, Kiyohiro IKEDA**, Takamasa SAKURAI*** and Akio HASEGAWA*****

This paper presents a total Lagrangian nonlinear formulation of elastic trusses, in which the governing stiffness equations are described as the relations between the overall forces and positions. With this selection of spatial positions as basic unknowns, the specification of the initial configuration becomes unnecessary and the separation of rigid body motion is automatically attained by an appropriate selection of local coordinates. A simple two bar truss and a reticulated truss are investigated as numerical examples. In the former, the characteristic of the present formulation and the convergence by the successive substitutions have been demonstrated. The latter example is chosen to show the effectiveness of the present formulation and simple systematic procedure to trace the finite displacement equilibrium paths including the main path and paths after bifurcations.

1. INTRODUCTION

Finite displacement problems for structural systems can be formulated discretely by the total Lagrangian method or by the up-dated Lagrangian method with unknown variables of nodal displacements[1)~15)] or nodal positions[16)]. The governing equations are expressed by the relations between the overall forces and displacements[4),16)] (or positions), or the relations between the incremental forces and incremental displacements[7)] (or positions) with[1),7),9)] or without[2),4)] the separation of rigid body displacements. The most popular among them seems to be the updated Lagrangian formulation with the separation of rigid body displacements in terms of the incremental forces and displacements.

Nonlinear discrete equations of structural systems can be solved numerically by the simple load incremental method without iteration[1)] or the iterative procedures such as the Newton-Raphson method[1)~3),6)] and the method of successive substitutions[1),8)]. The simple load incremental method is the easiest for mathematical manipulation, but may result in the accumulative errors in computation. The Newton-Raphson method produces second-order convergence[17)] when the tangent stiffness matrix is nonsingular. The direct solution of the governing equations by successive substitutions is simple in the iterative procedure. However, one of the drawbacks of the method of successive substitutions is that, unlike the Newton-Raphson method, the existence of convergence region is not guaranteed in the neighborhood of the solution and that it produces first-order convergence[17)], even when the solution converges.

Singular points of equilibrium such as bifurcation points can be analysed using the methods of eigen values[8)~11)],

* Member of JSCE, Ph. D., Professor of Civil Engineering University of Tokyo (Bunkyo-ku, Tokyo)
** Member of JSCE, M. Eng., Research Assistant, Tehnological University of Nagaoka (Nagaoka, Niigata)
*** Member of JSCE, M. Eng., Associate Professor of Civil Engineering, Toyota Technical College (Toyota, Aichi)
**** Member of JSCE, D. Eng., Associate Professor of Civil Engineering, University of Tokyo (Bunkyo-ku, Tokyo)

perturbations[10),12),13)] or initial imperfections[7),10)]. The perturbation method is most useful in the theoretical investigation of the behavior near bifurcation points, however, few numerical solutions have been tried only for simple problems since tedius and cumbersome computations are inevitable. The method of initial imperfections appears physically tractable and has been used for the analysis of simple structural systems[7),10)]. But solutions are found only in a heuristic sense, and no versatile procedure has been established in assuming the configurations of initial imperfections that will trace the most critical equilibrium path.

The use of eigen values may be most advantageous and versatile to determine bifurcation points and to trace the equilibrium paths branching out from the points, however, few studies have been made so far[14),15)].

This paper presents a total Lagrangian nonlinear formulation of elastic trusses, in which the governing stiffness equations are described as the relations between the overall forces and positions. With this selection of spatial positions as basic unknowns, the specification of the initial configuration becomes unnecessary and the separation of rigid body motion is automatically attained by an appropriate selection of local coordinates. The stiffness equations are solved numerically by the method of successive substitutions. This iterative procedure helped by the nature of the stiffness matrix obtained in this study is proved to be the same as the Newton-Raphson method.

2. STIFFNESS EQUATIONS OF TRUSSES

Consider a structural member pq with the initial undeformed length l subject to axial force only. Fig. 1 shows the member in equilibrium in a displaced state, for which the initial position of the member is of no importance. Superscripts p and q denote quantities at the ends p and q of the member, respectively.

Three rectangular Cartesian coordinates (x_1, x_2, x_3), $(x_{\bar{1}}, x_{\bar{2}}, x_{\bar{3}})$ and $(x_{\hat{1}}, x_{\hat{2}}, x_{\hat{3}})$ defined at the displaced state with the orthogonal base vectors $\{\boldsymbol{i}_i\}=\{\boldsymbol{i}_1\ \boldsymbol{i}_2\ \boldsymbol{i}_3\}$, $\{\boldsymbol{i}_{\bar{i}}\}=\{\boldsymbol{i}_{\bar{1}}\ \boldsymbol{i}_{\bar{2}}\ \boldsymbol{i}_{\bar{3}}\}$ and $\{\boldsymbol{i}_{\hat{i}}\}=\{\boldsymbol{i}_{\hat{1}}\ \boldsymbol{i}_{\hat{2}}\ \boldsymbol{i}_{\hat{3}}\}$, respectively, are introduced to describe a point in space.

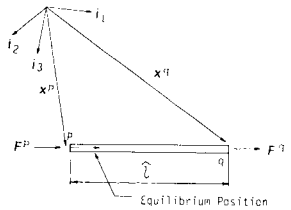

Fig. 1 A displaced member.

The bracket $\{\ \}$ indicates a column matrix. The base vector $\{\boldsymbol{i}_i\}$ is the reference frame fixed in space, whereas $\{\boldsymbol{i}_{\hat{i}}\}$ is the reference frame with $\boldsymbol{i}_{\hat{1}}$ selected along the member from p to q at the displaced equilibrium state and hence $\{\boldsymbol{i}_{\hat{i}}\}$ are generally unknown base vectors. The base vector $\{\boldsymbol{i}_{\bar{i}}\}$ is the reference frame selected to satisfy the condition

$$\boldsymbol{i}_{\bar{i}}\cdot\boldsymbol{i}_{\hat{i}}=\delta_{\bar{i}\hat{i}} \quad (1)$$

The position of each end of the member is expressed by the coordinates as

$$\left.\begin{aligned}\boldsymbol{x}^a&=\{x_1^a\ x_2^a\ x_3^a\}\\ \bar{\boldsymbol{x}}^a&=\{x_{\bar{1}}^a\ x_{\bar{2}}^a\ x_{\bar{3}}^a\}\\ \hat{\boldsymbol{x}}^a&=\{x_{\hat{1}}^a\ x_{\hat{2}}^a\ x_{\hat{3}}^a\}\end{aligned}\right\}\ a=p,q \quad (2\cdot\text{a}\sim\text{c})$$

The components of the force acting at one end of the member pq for the respective coordinates are defined as

$$\left.\begin{aligned}\boldsymbol{F}^a&=\{F_1^a\ F_2^a\ F_3^a\}\\ \bar{\boldsymbol{F}}^a&=\{F_{\bar{1}}^a\ F_{\bar{2}}^a\ F_{\bar{3}}^a\}\\ \hat{\boldsymbol{F}}^a&=\{F_{\hat{1}}^a\ F_{\hat{2}}^a\ F_{\hat{3}}^a\}\end{aligned}\right\}\ a=p,q \quad (3\cdot\text{a}\sim\text{c})$$

Consider the case that the member pq is subjected only to the end forces. Equilibrium equations are then given by

$$\left.\begin{aligned}\hat{\boldsymbol{F}}^p&=\{-N\ 0\ 0\}\\ \hat{\boldsymbol{F}}^q&=\{N\ 0\ 0\}\end{aligned}\right\} \quad (4\cdot\text{a, b})$$

in which N is the internal axial force in a member, which is a constant quantity along the length. Assume the material is elastic and governed by the following constitutive equation

$$N=EA(\hat{l}-l)/l \quad (5)$$

in which E, A and $\hat{l}$ are modulus of elasticity, initial undeformed cross sectional area and displaced length of the

member, respectively. Strain position relation is given by

$$\hat{l}=x_1^q-x_1^p=\sqrt{\{\overline{x}^q-\overline{x}^p\}^t\{\overline{x}^q-\overline{x}^p\}}=\sqrt{\{x^q-x^p\}^t\{x^q-x^p\}} \quad (6\cdot a)$$

or in vector form

$$\hat{l}\{i_1\}=(x_1^q-x_1^p)\{i_1\}=\{\overline{x}^q-\overline{x}^p\}^t\{i_{\bar{i}}\}=\{x^q-x^p\}^t\{i_i\} \quad (6\cdot b)$$

in which superscript t indicates transpose of a matrix.

Noting the direction cosine between $i_{\bar{i}}$ and $i_{\bar{i}}$ is expressed, in view of Eq. (6·b), by $(x_i^q-x_i^p)/\hat{l}$, the equilibrium equation (4) is transformed into

$$\overline{F}=-\begin{pmatrix}N\\ \hat{l}\end{pmatrix}\begin{Bmatrix}\overline{x}^q-\overline{x}^p\\ -\overline{x}^q+\overline{x}^p\end{Bmatrix}\begin{pmatrix}N\\ \hat{l}\end{pmatrix}\boldsymbol{K}^0\overline{x} \quad (7)$$

in which

$$\overline{F}=\begin{Bmatrix}\overline{F}^p\\ \overline{F}^q\end{Bmatrix},\qquad \overline{x}=\begin{Bmatrix}\overline{x}^p\\ \overline{x}^q\end{Bmatrix} \quad (8\cdot a,\ b)$$

$$\boldsymbol{K}^0=\begin{bmatrix}1&0&0&-1&0&0\\0&1&0&0&-1&0\\0&0&1&0&0&-1\\-1&0&0&1&0&0\\0&-1&0&0&1&0\\0&0&-1&0&0&1\end{bmatrix} \quad (9)$$

The matrix $\boldsymbol{K}^0$ is decomposed to the sum of the matrix $\boldsymbol{K}^1$ corresponding to small displacement theory and the remaining part $\boldsymbol{K}^2$ as

$$\boldsymbol{K}^0=\boldsymbol{K}^1+\boldsymbol{K}^2 \quad (10)$$

in which

$$\boldsymbol{K}^1=\begin{bmatrix}1&0&0&-1&0&0\\0&0&0&0&0&0\\0&0&0&0&0&0\\-1&0&0&1&0&0\\0&0&0&0&0&0\\0&0&0&0&0&0\end{bmatrix} \quad (11\cdot a)$$

$$\boldsymbol{K}^2=\begin{bmatrix}0&0&0&0&0&0\\0&1&0&0&-1&0\\0&0&1&0&0&-1\\0&0&0&0&0&0\\0&-1&0&0&1&0\\0&0&-1&0&0&1\end{bmatrix} \quad (11\cdot b)$$

Substituting Eq. (10) into Eq. (7) and making use of Eq. (5) lead to the stiffness equation of the member as

$$\overline{F}=\overline{K}\overline{x}-\overline{F}^0 \quad (12)$$

in which

$$\overline{F}^0=(EA/\hat{l})\boldsymbol{K}^1\overline{x} \quad (13)$$

$$\overline{K}=(EA/l)\boldsymbol{K}^1+(N/\hat{l})\boldsymbol{K}^2 \quad (14\cdot a)$$

In view of Eqs. (5) and (10), $\overline{K}$ can also be written as

$$\overline{K}=(EA/\hat{l})\boldsymbol{K}^1+(N/\hat{l})\boldsymbol{K}^0 \quad (14\cdot b)$$

Noting $x_1^q-x_1^p=\hat{l}$ and $x_2^q-x_2^p=x_3^q-x_3^p=0$, the selection of $\{i_{\bar{i}}\}$ equal to $\{i_i\}$ results in

$$\boldsymbol{K}^2\overline{x}=\boldsymbol{K}^2\hat{x}=0 \quad (15)$$

$$\overline{F}^0=\hat{F}^0=EA\{-1\ \ 0\ \ 0\ \ 1\ \ 0\ \ 0\} \quad (16)$$

and hence Eq. (12) becomes

$$\overline{F}=(\overline{E}A/l)\boldsymbol{K}^1\overline{x}-EA\{-1\ \ 0\ \ 0\ \ 1\ \ 0\ \ 0\} \quad (17)$$

in which $\hat{\boldsymbol{F}}^0$ and $\hat{\boldsymbol{x}}$ are quantities similar to $\overline{\boldsymbol{F}}^0$ and $\overline{\boldsymbol{x}}$ but defined in reference frame of $\{\boldsymbol{i}_{\tilde{\imath}}\}$.

The coordinate transformation matrix $\boldsymbol{T}$ relating $\boldsymbol{x}$ and $\boldsymbol{F}$ defined in the reference frame of $\{\boldsymbol{i}_i\}$ with $\overline{\boldsymbol{x}}$ and $\overline{\boldsymbol{F}}$, respectively, by

$$\overline{\boldsymbol{x}}=\boldsymbol{T}\boldsymbol{x},\quad \overline{\boldsymbol{F}}=\boldsymbol{T}\boldsymbol{F} \qquad (18\cdot a, b)$$

is given by

$$\boldsymbol{T}=(t_{\tilde{\imath}i})=\begin{bmatrix}[L_{\tilde{\imath}i}] & \boldsymbol{0}\\ \boldsymbol{0} & [L_{\tilde{\imath}i}]\end{bmatrix} \qquad (19)$$

in which

$$L_{\tilde{\imath}i}=\boldsymbol{i}_{\tilde{\imath}}\cdot\boldsymbol{i}_i \qquad (20)$$

Substituting Eq. (18) into Eq. (12) results in stiffness equation of the member in coordinate system fixed in space as

$$\boldsymbol{F}=\boldsymbol{K}\boldsymbol{x}-\boldsymbol{F}^0 \qquad (21)$$

in which

$$\boldsymbol{K}=\boldsymbol{T}^t\overline{\boldsymbol{K}}\boldsymbol{T} \qquad (22)$$

$$\boldsymbol{F}^0=(EA/\hat{l})\boldsymbol{T}^t\boldsymbol{K}^1\boldsymbol{T}\boldsymbol{x}=(EA/\hat{l})\boldsymbol{T}^t\boldsymbol{K}^1\boldsymbol{T}\boldsymbol{x}=(EA/\hat{l})<t_{\tilde{1}i}>^t<t_{\tilde{1}i}>\boldsymbol{x} \qquad (23)$$

with

$$<t_{\tilde{1}i}>=<L_{\tilde{1}1}\ L_{\tilde{1}2}\ L_{\tilde{1}3}\ -L_{\tilde{1}1}\ -L_{\tilde{1}2}\ -L_{\tilde{1}3}> \qquad (24)$$

The notation $<\ >$ indicates a row matrix. Making use of Eq. (14·a), $\boldsymbol{K}$ is expressed as

$$\boldsymbol{K}=(EA/l)<t_{\tilde{1}i}>^t<t_{\tilde{1}i}>+(N/\hat{l})\boldsymbol{T}^t\boldsymbol{K}^2\boldsymbol{T} \qquad (25\cdot a)$$

while use of q. (14·b) results in

$$\boldsymbol{K}=(EA/\hat{l})<t_{\tilde{1}i}>^t<t_{\tilde{1}i}>+(N/\hat{l})\boldsymbol{K}^0 \qquad (25\cdot b)$$

When $\{\boldsymbol{i}_{\tilde{1}}\}$ is selected to satisfy Eq. (1), there follows

$$x_{\tilde{1}}^q-x_{\tilde{1}}^p\fallingdotseq x_1^q-x_1^p=\hat{l} \qquad (26)$$

Then, noting the relation

$$\boldsymbol{K}^1\overline{\boldsymbol{x}}/\hat{l}=<-(x_{\tilde{1}}^q-x_{\tilde{1}}^p)/\hat{l}\ 0\ 0\ (x_{\tilde{1}}^q-x_{\tilde{1}}^p)/\hat{l}\ 0\ 0>^t\fallingdotseq<-1\ \ 0\ \ 0\ \ 1\ \ 0\ \ 0>^t \qquad (27)$$

$\boldsymbol{F}^0$ of Eq. (23) is expressed as

$$\boldsymbol{F}^0\fallingdotseq -EA<t_{\tilde{1}i}>^t \qquad (28)$$

When $\{\boldsymbol{i}_{\tilde{1}}\}$ is selected equal to $\{\boldsymbol{i}_{\hat{1}}\}$, substitution of Eq. (18) into Eq. (17) results in the stiffness equation of the form of Eq. (21) with $\boldsymbol{K}$ and $\boldsymbol{F}^0$ given by

$$\boldsymbol{K}=(EA/l)<t_{\hat{1}i}>^t<t_{\hat{1}i}> \qquad (29)$$

$$\boldsymbol{F}^0=-EA<t_{\hat{1}i}>^t \qquad (30)$$

in which $<t_{\hat{1}i}>$ is the row matrix defined in the same way as for $<t_{\tilde{1}i}>$, which is expressed by taking scalar product of Eq. (6·b) with $\boldsymbol{i}_i$ as

$$<t_{\hat{1}i}>=\frac{1}{\hat{l}}<|\boldsymbol{x}^q-\boldsymbol{x}^p|^t\ \ -|\boldsymbol{x}^q-\boldsymbol{x}^p|^t> \qquad (31)$$

Noting the direction cosine between $\boldsymbol{i}_{\hat{1}}$ and $\boldsymbol{i}_i$ is expressed by $(x_i^q-x_i^p)/\hat{l}$, the equilibrium equation (4) can also be expressed in terms of global coordinates as

$$\boldsymbol{F}=-\left(\frac{N}{\hat{l}}\right)\begin{Bmatrix}\boldsymbol{x}^q-\boldsymbol{x}^p\\ -(\boldsymbol{x}^q-\boldsymbol{x}^p)\end{Bmatrix} \qquad (32)$$

Substituting Eqs. (5) and (6·a), the governing equation in global coordinates is, then, expressed as

$$\boldsymbol{F}=-EA\left[\frac{1}{l}-\frac{1}{\sqrt{|\boldsymbol{x}^q-\boldsymbol{x}^p|^t|\boldsymbol{x}^q-\boldsymbol{x}^p|}}\right]\cdot\begin{Bmatrix}\boldsymbol{x}^q-\boldsymbol{x}^p\\ -(\boldsymbol{x}^q-\boldsymbol{x}^p)\end{Bmatrix} \qquad (33)$$

Differentiation of $\boldsymbol{F}$ with respect to $\boldsymbol{x}$ gives

$$d\boldsymbol{F}=\boldsymbol{K}_T(\boldsymbol{x})\,d\boldsymbol{x} \qquad (34)$$

in which

$$\boldsymbol{K}_T(\boldsymbol{x})=-\frac{EA}{(|\boldsymbol{x}^q-\boldsymbol{x}^p|^t|\boldsymbol{x}^q-\boldsymbol{x}^p|)^{3/2}}\cdot\begin{Bmatrix}\boldsymbol{x}^q-\boldsymbol{x}^p\\-(\boldsymbol{x}^q-\boldsymbol{x}^p)\end{Bmatrix}\begin{Bmatrix}\boldsymbol{x}^q-\boldsymbol{x}^p\\-(\boldsymbol{x}^q-\boldsymbol{x}^p)\end{Bmatrix}^t+\frac{N}{(|\boldsymbol{x}^q-\boldsymbol{x}^p|^t|\boldsymbol{x}^q-\boldsymbol{x}^p|)^{1/2}}\boldsymbol{K}^0 \quad (35)$$

By making use of Eq. (31) and Eq. (6·a), governing equation (33) and the tangential stiffness of Eq. (35) can be written as

$$\boldsymbol{F}=-EA|(\hat{l}-l)/l|<\boldsymbol{i}_{\hat{1}i}>^t \quad (36)$$

$$\boldsymbol{K}_T=(EA/\hat{l})<\boldsymbol{i}_{\bar{1}i}>^t<\boldsymbol{i}_{\bar{1}i}>+(N/\hat{l})\boldsymbol{K}^0 \quad (37)$$

Comparing Eq. (37) with Eq. (25·b), it can be noted that, when $\boldsymbol{i}_{\bar{1}}$ converges to $\boldsymbol{i}_{\hat{1}}$ and hence $<\boldsymbol{i}_{\bar{1}i}>$ to $<\boldsymbol{i}_{\hat{1}i}>$, the stiffness matrix of the nonlinear stiffness equation (21) becomes equal to the tangent stiffness of the same system.

The stiffness matrix of Eq. (14·a) consists with the constant matrix $(EA/l)\boldsymbol{K}^1$ corresponding to the stiffness matrix of small displacement and the matrix of a function of position $[N(\boldsymbol{x})/\hat{l}\,]\boldsymbol{K}^2$ corresponding to the geometric matrix. Since this expression of the stiffness matrix with these two terms agrees with the customary expressions, the expression of Eq. (14·a) seems to be the most natural choice. In this paper, however, an alternative expression is given in Eq. (14·b). When stiffness equation is transformed into global coordinate system, these stiffness matrices are expressed by Eqs. (25·a) and (25·b), respectively.

The customary expression of the stiffness matrix involves transformation matrix $\boldsymbol{T}$ defined between all three components of $|\boldsymbol{i}_{\bar{1}}|$ and those of $|\boldsymbol{i}_i|$. While the alternative expression involves only the transformation vector of Eq. (24) between $\boldsymbol{i}_{\bar{1}}$ and three components of $|\boldsymbol{i}_i|$. In view of Eqs. (23) and (25·b), it is obvious that, in the formulation of the member stiffness equation (21), the selection of base vectors $\boldsymbol{i}_{\bar{2}}$ and $\boldsymbol{i}_{\bar{3}}$ is trivial. It seems natural that quantities irrelevant to the final result are to be excluded in the formulation of the governing equation. By this reason, the stiffness matrices of Eqs. (25·b) and hence (14·b) are preferred in this paper and being used in the following numerical analysis.

It is noted that, when $|\boldsymbol{i}_{\bar{1}}|$ is selected to be equal to $|\boldsymbol{i}_{\hat{1}}|$, the stiffness equation for finite displacement of trusses becomes equal to that for small displacement as obvious from Eqs. (29) and (30).

The stiffness equation for a whole truss is obtained by the standard superposition procedure by making use of the equilibrium of forces and continuity of position at each nodal point.

3. ITERATIVE PROCEDURE BY SUCCESSIVE SUBSTITUTIONS

The nonlinear stiffness equation of a truss has been expressed in the form of Eq. (21). In view of Eq. (6), the unit vector $\boldsymbol{i}_{\hat{1}}$ in the direction of the displaced member is given by

$$\boldsymbol{i}_{\hat{1}}=|\boldsymbol{x}^q-\boldsymbol{x}^p|^t|\boldsymbol{i}_i|/\sqrt{|\boldsymbol{x}^q-\boldsymbol{x}^p|^t|\boldsymbol{x}^q-\boldsymbol{x}^p|} \quad (38)$$

Considering iterative solution for Eq. (21), position vectors after ν-th iteration are denoted by $(\boldsymbol{x}^p)^\nu$ and $(\boldsymbol{x}^q)^\nu$. The ν-th unit base vector $(\boldsymbol{i}_{\bar{1}})^\nu$ for the $(\nu+1)$-th iterative solution may, then, be chosen as

$$(\boldsymbol{i}_{\bar{1}})^\nu=|(\boldsymbol{x}^q)^\nu-(\boldsymbol{x}^p)^\nu|^t|\boldsymbol{i}_i|/\sqrt{|(\boldsymbol{x}^q)^\nu-(\boldsymbol{x}^p)^\nu|^t|(\boldsymbol{x}^q)^\nu-(\boldsymbol{x}^p)^\nu|} \quad (39)$$

This procedure is performed on each component member of the whole truss. When solution converges, comparison of Eqs. (38) and (39) shows that the condition of Eq. (1) is automatically satisfied. With $(\boldsymbol{i}_{\bar{1}})^\nu$ determined by Eq. (39), the coordinate transformation vector $<\boldsymbol{i}_{\bar{1}i}>^\nu$ as defined by Eq. (24) is expressed by

$$<\boldsymbol{i}_{\bar{1}i}>^\nu=<|(\boldsymbol{x}^q)^\nu-(\boldsymbol{x}^p)^\nu|^t \quad -|(\boldsymbol{x}^q)^\nu-(\boldsymbol{x}^p)^\nu|>/\sqrt{|(\boldsymbol{x}^q)^\nu-(\boldsymbol{x}^p)^\nu|^t|(\boldsymbol{x}^q)^\nu-(\boldsymbol{x}^p)^\nu|} \quad (40)$$

The force and position vectors consisting of the nodal points of the whole truss are denoted henceforth by the same notations as for the member element.

To utilize the method of successive substitutions, Eq. (21) is solved for $\boldsymbol{x}$ as

$$\boldsymbol{x}=[\boldsymbol{K}(\boldsymbol{x})]^{-1}|\boldsymbol{F}+\boldsymbol{F}^0(\boldsymbol{x})| \quad (41)$$

and successive estimates of the solution are determined using

$$\boldsymbol{x}^{\nu+1}=[\boldsymbol{K}(\boldsymbol{x}^\nu)]^{-1}|\boldsymbol{F}+\boldsymbol{F}^0(\boldsymbol{x}^\nu)| \quad (42)$$

Unlike the Newton-Raphson method, the method of successive substitutions does not assure convergence, and only produces first-order convergence in general, even if the solution converges[17]. When the successive substitutions

converge, $\boldsymbol{i}_{\hat{1}}$ also converges to $\boldsymbol{i}_{\hat{1}}$ and hence either of the expressions of Eqs. (25) and (29) may be used for the stiffness matrix $\boldsymbol{K}$ in Eq. (42).

The Newton-Raphson procedure for Eq. (33) under the given force $\boldsymbol{F}$ is expressed by[17]

$$\boldsymbol{x}^{\nu+1}=\boldsymbol{x}^{\nu}-[-\boldsymbol{K}_T(\boldsymbol{x}^{\nu})]^{-1}\cdot\{\boldsymbol{F}+EA[\hat{l}(\boldsymbol{x}^{\nu})/l-1]<t_{\hat{1}i}(\boldsymbol{x}^{\nu})>^t\} \quad (43)$$

with $\boldsymbol{K}_T$ of Eq. (37). Using Eq. (5) and the following identities

$$(N/\hat{l})\boldsymbol{K}^0\boldsymbol{x}=-N<t_{\hat{1}i}>^t \quad (44)$$

$$<t_{\hat{1}i}>\boldsymbol{x}=-\hat{l} \quad (45)$$

Eq. (37) post-multiplied with $\boldsymbol{x}$ yields

$$\boldsymbol{K}_T\boldsymbol{x}=-EA(\hat{l}/l)<t_{\hat{1}i}>^t \quad (46)$$

from which

$$\boldsymbol{x}^{\nu}=-[EA\hat{l}(\boldsymbol{x}^{\nu})/l][\boldsymbol{K}_T(\boldsymbol{x}^{\nu})]^{-1}<t_{\hat{1}i}(\boldsymbol{x}^{\nu})>^t \quad (47)$$

Substituting Eq. (47) and Eq. (37) into Eq. (43) results in

$$\boldsymbol{x}^{\nu+1}=\left[\frac{EA}{\hat{l}(\boldsymbol{x}^{\nu})}<t_{\hat{1}i}(\boldsymbol{x}^{\nu})>^t<t_{\hat{1}i}(\boldsymbol{x}^{\nu})>+\frac{N}{\hat{l}(\boldsymbol{x}^{\nu})}[\boldsymbol{K}^0]^{-1}\right]\{\boldsymbol{F}-EA<t_{\hat{1}i}(\boldsymbol{x}^{\nu})>^t\} \quad (48)$$

Noting that ν-th estimate $<t_{\hat{1}i}(\boldsymbol{x}^{\nu})>$ is nothing but $<t_{\hat{1}i}(\boldsymbol{x}^{\nu})>$ and that Eq. (28) holds when Eq. (39) converges to Eq. (38), the successive substitutions of Eq. (42) when the stiffness matrix of Eq. (25·b) is employed is identical to the Newton-Raphson procedure of Eq. (48) and hence of Eq. (43). Accordingly, under the given force, $\boldsymbol{F}$, the successive substitutions of Eq. (42) with $\boldsymbol{K}$ of Eq. (25) guarantee second-order convergence for an initial value sufficiently close to the true solution $\boldsymbol{x}$.

For the most general numerical treatment, the force vector $\boldsymbol{F}$ is expressed by the product of constant vector $\boldsymbol{f}$ and varible scalar f as

$$\boldsymbol{F}=f\boldsymbol{f} \quad (49)$$

By specifying the values of $\boldsymbol{x}^{\nu}$, Eq. (42) or its original form, Eq. (21), when Eq. (49) is substituted, constitutes linear simultaneous equations with unknowns $\boldsymbol{x}^{\nu+1}$ and $f^{\nu+1}$, which can be written as

$$[\boldsymbol{K}(\boldsymbol{x}^{\nu}) \quad -\boldsymbol{f}]\begin{Bmatrix}\boldsymbol{x}^{\nu+1}\\ f^{\nu+1}\end{Bmatrix}-\boldsymbol{F}^0(\boldsymbol{x}^{\nu})=0 \quad (50)$$

Since the number of unknowns is larger by one than that of the equations, an additional condition must be introduced among variables $\boldsymbol{x}$ and f. In structural analysis, it is common that nodal positions of structures are solved under the given force as expressed by

$$f-c_{j+1}=0 \quad (51)$$

where c_{j+1} is a constant for $(j+1)$-th solution. While, so-called position control or path length control[14] is also used in nonlinear structural analysis. In the former, one of the positions, for example x_i, is given as

$$x_i-c_{j+1}=0 \quad (52)$$

In the latter, a path length of equilibrium curve in $n+1$ dimensional space is given as

$$\sum_{i=1}^{n}a_i^2(x_i-x_i^0)^2+a_{n+1}^2(f-f^0)^2-c_{j+1}^2=0 \quad (53)$$

in which f^0 and x_i^0 are the known components of j-th solution on the equilibrium curve. The a_1 up to a_n are non-dimensional arbitrary constants, while a_{n+1} is another arbitrary constant equating the dimension of f to that of x_i.

It is noted that Eqs. (51) and (52) are the special cases of Eq. (53). From this, it is obvious that to retain all of the left side terms of Eq. (53) is not necessary and some of the terms may be discarded arbitarily by selecting a_i being equal to zero. The magnitude of a_i may be selected on trial basis for a faster convergence. With no information available for appropriate magnitudes, unity or zero may be assigned for a_1 up to a_n, while the magnitude of a_{n+1} may be selected such that the order of $a_{n+1}|f-f^0|$ becomes equal to that of the largest element of $|x_i-x_i^0|$ at the range where linear small displacement theory holds.

Since Eq. (53) is nonlinear, it may be linearlized for the purpose of iteration. Expanding in Taylor series about the ν-th estimates, x_i^{ν} and f^{ν}, and retaining only linear terms, Eq. (53) becomes

$$\left\{\sum_{i=1}^{n} a_i^2(x_i^\nu-x_i^0)^2+a_{n+1}^2(f^\nu-f^0)^2-c_{j+1}^2\right\}+2\left\{\sum_{i=1}^{n} a_i^2(x_i^\nu-x_i^0)(x_i^{\nu+1}-x_i^\nu)+a_{n+1}^2(f^\nu-f^0)(f^{\nu+1}-f^\nu)\right\}=0 \cdots\cdots (54)$$

With the specification of one additional condition, the $n+1$ unknowns $\boldsymbol{x}$ and f may be solved by iteration. Combining Eq. (54) with Eq. (50), successive estimates of the solution are determined by

$$\begin{Bmatrix} \boldsymbol{x}^{\nu+1} \\ f^{\nu+1} \end{Bmatrix}=\begin{bmatrix} \boldsymbol{K}(\boldsymbol{x}^\nu) & -\boldsymbol{f} \\ \boldsymbol{K}_{n+1}(\boldsymbol{x}^\nu) & a_{n+1}^2(f^\nu-f^0) \end{bmatrix}^{-1}\cdot\begin{Bmatrix} \boldsymbol{F}^0(\boldsymbol{x}^\nu) \\ F_{n+1}^0(\boldsymbol{x}^\nu,f^\nu) \end{Bmatrix} \cdots\cdots (55)$$

where

$$\boldsymbol{K}_{n+1}(\boldsymbol{x}^\nu)=<a_1^2(x_1^\nu-x_1^0)\quad a_2^2(x_2^\nu-x_2^0)\cdots a_n^2(x_n^\nu-x_n^0)> \cdots\cdots (56)$$

$$F_{n+1}^0(\boldsymbol{x}^\nu,f^\nu)=\left\{\sum_{i=1}^{n} a_i^2(x_i^\nu-x_i^0)x_i^\nu+a_{n+1}^2(f^\nu-f^0)f^\nu\right\}-\frac{1}{2}\left\{\sum_{i=1}^{n} a_i^2(x_i^\nu-x_i^0)^2+a_{n+1}^2(f^\nu-f^0)^2-c_{j+1}^2\right\} \cdots\cdots (57)$$

By similar treatment as for the derivation of Eq. (48), it can be shown that successive substitutions of Eq. (55) is identical to the Newton-Raphson procedure of $n+1$ nonlinear simultaneous equations (33) and (53).

From the view point of convergence, it is advantageous to employ Newton-Raphson iteration than other iterative procedure. An alternative process may also be employed, however, by dividing the iterative process of Eq. (55) into two processes. With $\boldsymbol{x}^\nu$ and f^ν, $\boldsymbol{x}^{\nu+1}$ is determined first by Eq. (42) and then $f^{\nu+1}$ is determined by substituting this $\boldsymbol{x}^{\nu+1}$ into either Eq. (53) or (54). Using Eq. (53), $f^{\nu+1}$ is given as

$$f^{\nu+1}=\sqrt{\frac{c_{j+1}^2-\sum_{i=1}^{n} a_i^2(x_i^{\nu+1}-x_i^0)^2}{a_{n+1}^2}}+f^0 \cdots\cdots (58)$$

This two step process may be in advantage at a point close to a stationary point for loading intensity, where $f-f^0$ becomes close to zero and hence the last diagonal term of the coefficient matrix of Eq. (55). Further, the symmetry of $\boldsymbol{K}(\boldsymbol{x}^\nu)$ is fully utilized in numerical computation. It is noted that this alternative iterative process is not identical with the Newton-Raphson process even if $f^{\nu+1}$ is determined from Eq. (54).

Selection of initial values is very important for the iterative procedure by two reasons. Firstly, it affects the efficiency of iteration in successive substitutions. Secondly, when equilibrium paths branch out from bifurcation points, the convergence of the solution into a point on the original equilibrium path or on the branch depends on the selection of initial values. Knowing the j-th solutions f^0 and $\boldsymbol{x}^0$, the initial values f^1 and $\boldsymbol{x}^1$ for the next $(j+1)$-th solutions can be selected by the sum of these solutions and their increments as

$$f^1=f^0+\Delta f^0,\quad \boldsymbol{x}^1=\boldsymbol{x}^0+\Delta\boldsymbol{x}^0 \cdots\cdots (59\cdot a, b)$$

Since the stiffness matrices of Eq. (25) coincide with the tangent stiffness of the system, the load increment and increments of positions are related as

$$\Delta f^0\,\boldsymbol{f}\fallingdotseq\boldsymbol{K}(\boldsymbol{x}^0)\Delta\boldsymbol{x}^0 \cdots\cdots (60)$$

The solution of Eq. (60), when the nearly equal sign is replaced with the equal sign, is given by[18]

$$\Delta\boldsymbol{x}^0=\sum_{i=1}^{n}\left(\frac{\boldsymbol{e}_i\cdot\boldsymbol{f}}{\lambda_i}\right)\Delta f^0\,\boldsymbol{e}_i \cdots\cdots (61)$$

where λ_i and $\boldsymbol{e}_i$ are the i-th eigen value and the corresponding normalized eigen vector of $\boldsymbol{K}(\boldsymbol{x}^0)$. Eq. (60) has an unique solution unless $\lambda_i=0$, that is, unless $\boldsymbol{K}(\boldsymbol{x}^0)$ is singular. The unique solution is given in a moae familiar form as

$$\Delta\boldsymbol{x}^0=\Delta f^0[\boldsymbol{K}(\boldsymbol{x}^0)]^{-1}\boldsymbol{f} \cdots\cdots (62)$$

When $\lambda_i=0$ where λ_i may be multiple roots, a solution of Eq. (60) exists only when $\boldsymbol{e}_i\cdot\boldsymbol{f}=0$ and/or $\Delta f^0=0$. When $\boldsymbol{e}_i\cdot\boldsymbol{f}\neq 0$, Δf^0 has to be equal to zero. The loading is then stationary at this equilibrium point $\boldsymbol{x}^0$ with respect to the variation of $\boldsymbol{x}$ and hence it is the maximum, the minimum or an inflexion point. Since $\Delta f^0\fallingdotseq 0$ at this stationary point, the increment $\Delta\boldsymbol{x}^0$ of Eq. (61) is expressed by a linear combination of eigen vector $\boldsymbol{e}_i$ corresponding to zero eigen values, $\lambda_i=0$, as

$$\Delta\boldsymbol{x}^0=\sum_i c_i\,\boldsymbol{e}_i \cdots\cdots (63)$$

where c_i is an arbitary constant. Eq. (63) is the homogeneous solution of Eq. (60) with $\Delta f^0=0$. When a solution

of Eq. (60) exists with nonzero Δf^0, $\boldsymbol{e}_i \cdot \boldsymbol{f}$ has to be equal to zero and hence Eq. (61) becomes

$$\Delta \boldsymbol{x}^0 = \sum_i c_i \boldsymbol{e}_i + \Delta \boldsymbol{x}^p \quad (64)$$

where $\Delta \boldsymbol{x}^p$ is a particular solution of Eq. (60) and may be given by

$$\Delta \boldsymbol{x}^p = \sum_{j=1}^{n} \left(\frac{\boldsymbol{e}_j \cdot \boldsymbol{f}}{\lambda_j} \right) \Delta f^0 \boldsymbol{e}_j \quad (j \neq i) \quad (65)$$

The fact that the solution $\Delta \boldsymbol{x}^0$ of Eq. (60) is not unique at a nonstationary point shows that the singular point is a bifurcation point of equilibrium.

Assigning an appropriate value to Δf^0, the initial estimate of f^1 and $\boldsymbol{x}^1$ for $(j+1)$-th solution are determined by Eqs. (59) together with (52). The value of Δf^0 is arbitrary, however, when no information is available for an appropriate value, it may be determined by the condition that the initial estimates of the increments satisfy the condition of Eq. (53). Substituting Eqs. (59) and (62) into Eq. (53) yields

$$(\Delta f^0)^2 = \frac{c_{i+1}^2}{\{[\boldsymbol{K}(\boldsymbol{x}^0)]^{-1} \boldsymbol{f}\}^2 [\boldsymbol{K}(\boldsymbol{x}^0)]^{-1} \boldsymbol{f}\} + a_{n+1}^2} \quad (66)$$

in which

$$\boldsymbol{a}^2 = <a_1^2 \ a_2^2 \cdots a_n^2> \quad (67)$$

At the end of each iteration, it is necessary to check the existence of singular points between the two neighbouring solutions, if there is any possibility. This can be done by checking the eigen values for the change of the sign between the two sufficiently close neighbouring solutions. With the presence of a possible bifurcation point, initial values may be determined with Eq. (63) or (64) whichever appropriate for a solution on the possible bifurcation path. When Eq. (63) is to be used to determine the initial values, the number of arbitrary parameter c_i is equal to the number of zero multiple roots at the singular point. When Eq. (64) is to be used, the number increases one more with Δf^0 as an additional arbitrary parameter. For these number of undetermined parameters, there exists only one condition, Eq. (53) or (54), which may be used to relate them. An appropriate value is to be assigned on trial basis to each of the undetermined parameters, c_i and Δf^0, or to each of them except one which is determined by Eq. (53) or (54).

Since the iterative process involves the computation of the inverse of $\boldsymbol{K}$, numerical computation may become unstable at a point close to a singular point when $\boldsymbol{K}$ of Eq. (25) is used. Generally, solutions at singular points or very close to them may not be necessary to trace equilibrium paths. If, however, a solution is required at a point so close to a singular point that the solution can not be obtained within a tolerable accuracy, iterative solution may be tried with the stiffness of Eq. (29). Since the matrix is the same with that of small displacement theory, it is nonnegative and hence it exhibits nosingularity except at the unstable geometrical configuration in the sense of small displacement theory of structural analysis. By this reason, a solution can be obtained even at a stationary point or at a bifurcation point by the use of $\boldsymbol{K}$ of Eq. (29), when the solution converges. Contrary to Newton-Raphson process, there is no guarantee for the convergence even for initial values sufficiently close to the true solution, however, the iterative process with $\boldsymbol{K}$ of Eq. (29) converges to a true solution when it converges.

4. NUMERICAL EXAMPLE OF A TWO-BAR TRUSS AND ITS CONVERGENCE

The convergence of Eq. (42) of the successive substitutions is examined for a two-bar truss as shown in Fig. 2. The truss is subject to only one external force F_1 at point Q in the i_1-direction and displacements are assumed to be symmetric with respect to the i_1-axis. Thus, the i_2-component x_2 of the position vector at point Q is identically equal to zero, and x_1 is the only one unknown. The successive substitutions of Eq. (42) for this truss becomes

$$x_1^{\nu+1} = [f + F^0(x_1^\nu)]/K(x_1^\nu) \quad (68)$$

When Eqs. (25·b) and (23) are employed, $K(x_1)$ and $F^0(x_1)$ are expressed as

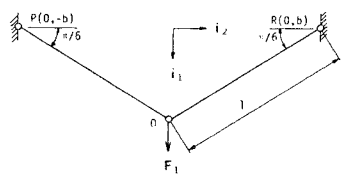

Fig. 2 A two-bar truss.

$$\left.\begin{aligned} K(x_1)&=(2EA/l)(1-b^2l/\hat{l}^3)\\ F^0(x_1)&=(2EA/\hat{l})(1-b^2/\hat{l}^2)x_1\\ \hat{l}&=\sqrt{b^2+x_1^2}\end{aligned}\right\} \cdots\cdots (69\cdot a\sim c)$$

While the employment of Eqs. (29) and (30) yields

$$\left.\begin{aligned} K(x_1)&=(2EA/l)(x_1^2/\hat{l}^2)\\ F^0(x_1)&=(2EA/\hat{l})(-1+\hat{l}+x_1^2/\hat{l}^2)x_1\end{aligned}\right\} \cdots\cdots (70\cdot a, b)$$

Regarding x_1^ν as known quantity, Eq. (68) is a linear relation between f and $x_1^{\nu+1}$. The exact relation of Eq. (33) for this truss between f and x_1 is given by

$$f=2EA\,x_1(1/l-1/\sqrt{b^2+x_1^2}) \cdots\cdots (71)$$

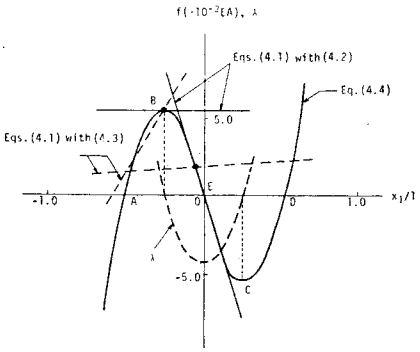

Fig. 3 Equilibrium path of a two-bar truss.

Fig. 3 shows graphically this exact equation (71) and the linear relation of Eq. (68) between f and $x_1^{\nu+1}$. In the latter, the points satisfying $x_1^{\nu+1}=x_1$ are marked by the dot (·) on the straight line of Eq. (68). These marked points are located on the equilibrium curve. This shows that the values (f, $x_1^{\nu+1}$) of Eq. (68) are identical with the solution of Eq. (71), if the successive substitutions converge.

As has been discussed earier, it is seen in Fig. 3 that the straight line of Eq. (68) with Eq. (69) becomes the tangent line to the exact equilibrium curve of Eq. (71) at the point satisfying $x_1^{\nu+1}=x_1$. On the other hand, the straight line of Eq. (68) with Eq. (70) is not the tangential line to Eq. (71). Further, the slope of this straight line is non-negative even for unstable regions of equilibrium, which is due to the non-negative property of the stiffness matrix.

Fig. 3 also includes the relation between x_1 and λ determined from $K(x_1)$ of Eq. (69·a). The degree of freedom of this truss is one, and hence there exists only one eigen value. As shown in the figure by a dotted line, the eigen value is equal to zero at the stationary points B and C. It is obvious that, by noting the change of sign of the eigen value at two neighbouring points, the presence of a singular point in between can easily be detected.

Convergence of the successive substitutions under the force f given is examined on this example. As discussed before, the successive substitutions of Eq. (68) with $K(x_1^\nu)$ of Eq. (69) produce second-order convegence for initial values sufficiently close to the true solution except at the singular points B and C. On the other hand, successive substitutions of Eq. (68) combined with $K(x_1^\nu)$ of Eq. (70) is not the Newton-Raphson iteration and hence there is no guarantee for convergence. The successive substitutions of Eq. (68) converges when the following inequality holds[17].

$$g(x_1)=\frac{d}{dx}\{[f+F^0(x_1)]/K(x_1)\}<1 \cdots\cdots (72)$$

Otherwise the solution diverges. Substituting Eq. (70), $g(x_1)$ is expressed as

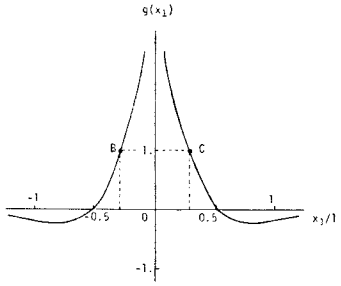

Fig. 4 Profile of $g(x_1)$.

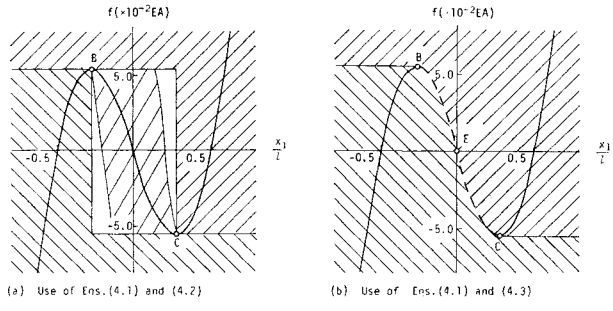

Fig. 5 Convergence regions.

$$g(x_1)=(b^2/x_1^2)(-1+l/\sqrt{x_1^2+b^2}) \quad \cdots\cdots (73)$$

Fig. 4 shows the relation between x_1 and $g(x_1)$ as given by Eq. (73). The figure indicates that the solutions diverge in the region of unstable equilibrium between points B and C and converges in the remaining region.

Fig. 5 shows the regions of the initial value x_1, with which the iterative process converges under a given force f. The solid lines of the equilibrium curve indicate the solution which the iterative process converges, while the dashed line is the solution which the iterative process can not converge regardless of the initial values. The shaded portion is the region of initial values with which solution converges to the solid line in that region and the open portion is the compound region of initial values, with which the iterative process converges to one of the three solutions depending on the location of the initial values in the region.

5. NUMERICAL EXAMPLE OF A RETICULATED TRUSS

A reticulated truss[2),10),14),15),19)] as shown in Fig. 6 is analysed as a numerical example with multi-degrees of freedom system. The solution is obtained by prescribing the path length of equilibrium using the stiffness matrix of Eq. (25·b).

Fig. 7 shows relations between loading intensity and vertical position of the node b of the truss for the loading pattern (a) as given in Table 1. The numerical results obtained by the present study are shown by dots. Also shown in the figure are the results by Hangai and Kawamata[10], Jagannathan, Epstein and Christiano[2] and Yoshida, Masuda, Morimoto and Hirosawa[19]. The analysis agrees well with the results of Yoshida et al. but differs remarkably from the others. It has been checked that the numerical results of this study satisfy the exact governing equation (33).

It was pointed by both Jagannathan et al. and Yoshida et al. that the curve should pass the origin again when $f=0$ and hence numerical errors are present in the analysis of Hangai et al. This configuration corresponds to the displacement of node a downward by 4 cm and no displacement at other nodes (see Fig. 9. (c)). It is obvious that the system is in self-equilibrium and hence f must be equal to zero at this configuration.

Jagannathan et al. assumed a linear constitutive relationship between the Kirchhoff's stress tensor and the Green's strain tensors, as expressed by

$$N=EA\left(\frac{\hat{l}}{N}\right)\left(\frac{\hat{l}^2-l^2}{2l^2}\right) \quad \cdots\cdots (74)$$

For comparison, numerical computations were made by the mehod of present analysis employing Eq. (74) as constitutive equation instead of Eq. (5). The results are plotted in Fig. 7 as indicated by triangles. There was difference between the solutions employing Eqs. (5) and (74), but, as can be seen in the figure, it was insignificant within the range of loaing and

Table 1 Vertical loading pattern.

Joint NO.	Pattern (a)	Pattern (b)
a	1.0	0.5
b	0.0	1.0
c	0.0	1.0
d	0.0	1.0
e	0.0	1.0
f	0.0	1.0
g	0.0	1.0

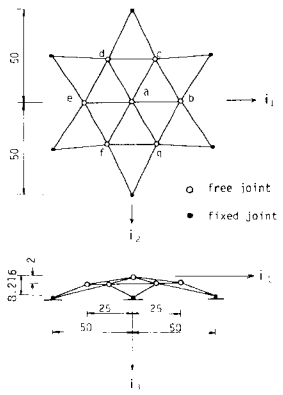

Fig. 6 A reticulated truss (unit in cm).

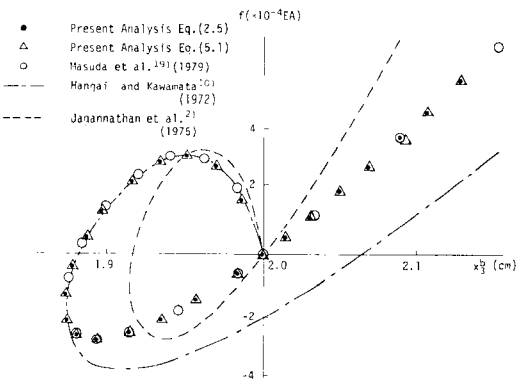

Fig. 7 Equilibrium path for loading pattern (a).

displacements of Fig. 7. These numerical results were also checked for the accuracy to satisfy the exact governing equation which can be obtained by substituting Eq. (74) into Eq. (32). The accuracy of the results by Jagannathan et al. may also be subject to question.

In order to demonstrate the numerical computation to find bifurcation points and bifurcated equilibrium paths, the reticulated truss is analysed for loading pattern (b) of Table 1[14,15]. The main equilibrium path starting from the initial configuration with symmetrical displacements is shown in Fig. 8 with the vertical position x_3^a of node a in the abscissa and the force intensity f in the ordinate. The eigen value analysis is performed to check the presence of possible singular points simultaneously with the determination of a point on the main equilibrium path. The singular points thus obtained are marked in the figure by symbols (Δ), (∇) and ($\square$) which indicate bifurcation points with a single root and multiple roots of zero, and stationary points, respectively. Fig. 9 shows the self-evident equilibrium configurations for $f=0$. These configurations correspond to points Q, R, S and P in Fig. 8. It may be worth to mention that this rather complex equilibrium path has been obtained by a single job of computation, detecting all the singular points.

The first portion of the equilibrium path of Fig. 8 is enlarged and depicted in Fig. 10. Aslo shown in Fig. 10 by dotted lines are the changes of the magnitude of each eigenvalue with the change of equilibrium configuration, where λ_i is the i-th smallest eigen value. Single dotted line for λ_2, λ_3 and that for λ_4, λ_5 show that both of them are

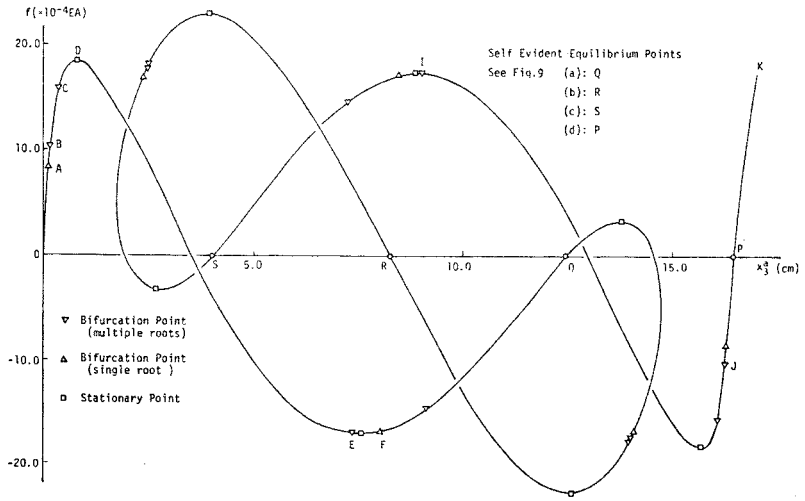

Fig. 8 Equilibrium path for loading pattern (b).

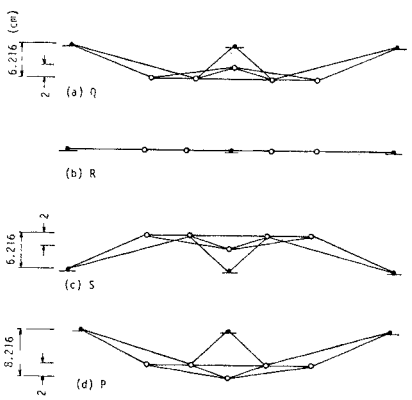

Fig. 9 Self-evident equilibrium configurations for $f=0$.

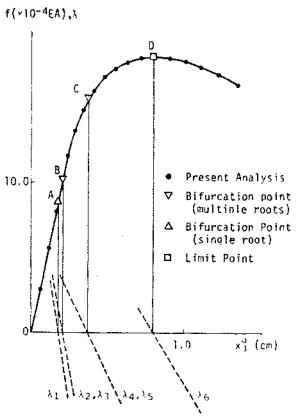

Fig. 10 Equilibrium path and eigenvalue curves.

double multiple roots. Singular points within the range of this figure on the main equilibrium path are points A, B, C and D, where the corresponding eigen values λ_1 through λ_6 are reduced to zero.

Table 2 shows the seven i_3-components of eigen vectors at points A, B, C and D. The other 14 components are small compared with unity and omitted to list in the Table. The value of $\boldsymbol{f}\cdot\boldsymbol{e}_i$ becomes zero at points A, B and C, whereas the value at point D is not reduced to zero. This shows that points A, B and C are bifurcation points and point D is a stationary point.

The method of successive substitutions is performed to compute bifurcated equilibrium paths using values of Eq. (59) with increment determined by Eq. (63) in which arbitrary constants c_i are determined on trial basis. The results are shown in Fig. 11 with positions x_3^b and x_3^c in the orthogonal horizontal axes and force intensity f in the vertical axis. In the figure, 0) indicates a portion of the main equilibrium path shown in Fig. 8, whereas A), B–1) ~ Be–3) and C–1) ~ C–6) indicate one, three and six bifurcated paths from points A, B and C, respectively.

Table 2 i_3-Components of eigen vectors at points A, B, C and D.

Point	A	B		C		D
Eigen Value	$\lambda_1=0$	$\lambda_2=0$,	$\lambda_3=0$	$\lambda_4=0$,	$\lambda_5=0$	$\lambda_6=0$
x_3^a	0.00	0.00	0.00	0.00	0.00	0.49
x_3^b	1.00	0.00	2.00	0.00	-2.00	1.00
x_3^c	-1.00	-1.00	-1.00	-1.00	-1.00	1.00
x_3^d	1.00	1.00	-1.00	-1.00	1.00	1.00
x_3^e	-1.00	0.00	2.00	0.00	2.00	1.00
x_3^f	1.00	-1.00	-1.00	1.00	1.00	1.00
x_3^g	-1.00	1.00	-1.00	1.00	-1.00	1.00

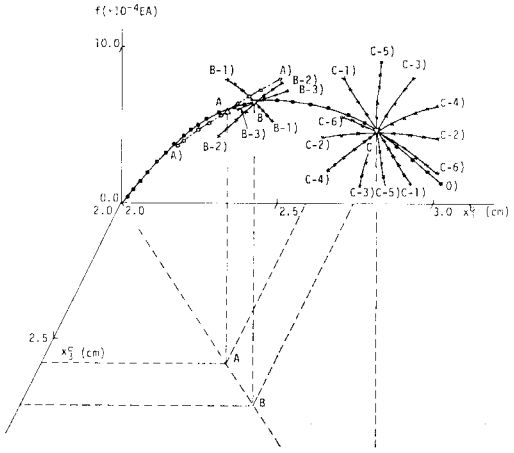

Fig. 11 Spatial sketch of equilibrium paths near bifurcation points.

Since points A, B and C are not the stationary points, Eq. (64) can also be used for the estimation of an increment. With this increment including the particular solution, however, the iterative solution showed a tendency to converge on a solution on the main equilibrium path, rather than on the bifurcated paths. The force increment at the bifurcation points in the direction of bifurcated paths are nearly equal to zero at A and C, whereas that is not so at B. This shows that the bifurcated paths at A and C are stationary at the bifurcation points, whereas those at B are not. These two types of bifurcated equilibrium paths are called as symmetric and asymmetric bifurcations, respecitively[12),14),15)]. Because of this, it is obvious that a better initial value for a solution on the bifurcated paths can be estimated at A and C by the homogeneous solution, but the particular solution represents the increment on the main equilibrium path.

The tangential vectors at each singuar points A through D are determined by the vector from the bifurcation point to a nearby point on the bifurcated equilibrium path, and their i_3-components are given in Table 3. Comparing Tables 2 and 3, it is seen that the modes of the tangential vectors agree with those of the eigen vectors or with their linear combinations at symmetric bifurcation points A and C where the force increment is equal to zero for bifurcation paths. On the other hand, the tangential vectors at asymmetric bifurcation point B where the force increment is not equal to zero can not be expressed by the linear combinations of the eigen vectors. This is obvious by the fact that the linear combination of the eigen vectors of Eq. (63) represents the homogeneous solution of Eq. (60) and hence it can not represent the mode of tangential vectors, $\Delta\boldsymbol{x}^0$, for asymmetric bifurcation in which Eq. (60) is not homogeneous. The non-homogeneous mode can be represented by Eq. (64) adding particular solution to the homogeneous solution. Whether a bifurcated path is symmetric or asymmetric is not known beforehand, but it becomes known only when solutions are obtained within the frame work of the present study. The behavior of the

Table 3 Tangents of equilibrium paths at points A, B, C and D.

Point	A	B			C						D
df	0	≒ 0			0						0
Path	A)	B-1)	B-2)	B-3)	C-1)	C-2)	C-3)	C-4)	C-5)	C-6)	D)
x_3^a	0.0	0.21	0.21	0.21	0.0	0.0	0.0	0.0	0.0	0.0	0.49
x_3^b	-1.0	1.0	1.0	0.98	1.0	1.0	0.0	1.0	-1.0	-1.99	1.0
x_3^c	1.0	1.0	0.98	1.0	1.0	0.0	-1.0	-1.0	-1.99	-1.0	1.0
x_3^d	-1.0	0.98	1.0	1.0	0.0	-1.0	-1.0	-1.99	-1.0	1.0	1.0
x_3^e	1.0	1.0	1.0	0.98	-1.0	-1.0	0.0	-1.0	1.0	1.99	1.0
x_3^f	-1.0	1.0	0.98	1.0	-1.0	0.0	1.0	1.0	1.99	1.0	1.0
x_3^g	1.0	0.98	1.0	1.0	0.0	1.0	1.0	1.99	1.0	-1.0	1.0

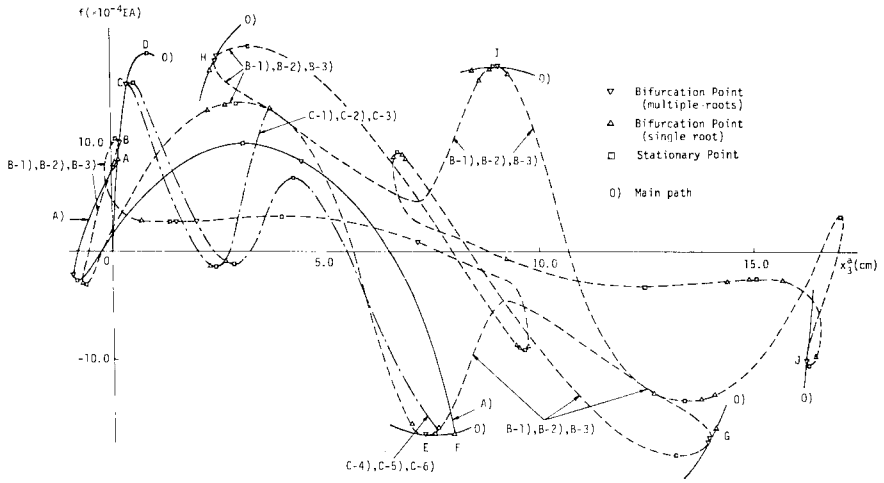

Fig. 12 Main equilibrium paths after bifurcations at A, B, and C.

bifurcated equilirium paths can be studied considering higer order differentials[12] with the expense of additional computaion. Whether the effort is worth for computing equilirium paths remains to be studied. Because of this, generally a trial for the selection of Eq. (63) or (64) is also necessary in addition to the trial selection of c_i for the choice of initial values to obtain solutions of a point on bifurcated paths.

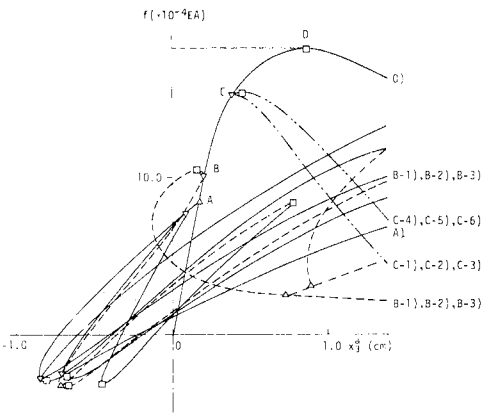

Fig. 13 Complete equilibrium paths near the initial configuration.

After the main equilibrium path as shown in Fig. 8 is traced, similar analysis can be performed next to trace the main paths of the bifurcated equilibrium paths from each bifurcation point. Those paths may be called as the second generation of the equilibrium curves. All of the main equilibrium paths, that is smooth continuous paths, bifurcated from points A, B and C are thus traced and shown in Fig. 12 selecting the position $x_3{}^a$ in the abscissa and the force intensity f in the ordinate. Although some of the bifurcated paths such as B–1) ~B–3) are identical when projected into this two dimensional plane of (f, $x_3{}^a$), those differ from each other in the 22-dimensional space of (f, x). Hosono[14),15)] has also computed the equilibriumpath bifurcated from the points A, B and C, but part of them.

After the main paths of the bifurcated paths from the original main path 0) are traced, similar analysis can be performed again to trace the bifurcated paths, that is, the third and further generations of the equilibrium curves from the bifurcation points on the second generation of the equilibrium curves as shown in Fig. 12. An example of this third generation curves is shown in Fig. 13 which depicts all the bifurcated paths within the range of $-1 < x_3{}^a < 1.4$.

6. CONCLUDING REMARKS

Although the up-dated Lagrangian formulations in terms of incremental forces and displacements are popular in general for the analysis of the finite displacement problems of structures, this paper presents a total Lagrangian formulation in terms of overall nodal forces and positions, which seems to be even simpler than up-dated Lagrangian formulation at least for the analysis of a truss. Use of nodal positions as basic unknown quantities instead of displacements is noted by two reasons. The first is that the formulation does not require any information on the initial configuration but only the dimensions of the members and continuity conditions of the nodes. It seems natural that quantities irrelevant to the final results are to be excluded in the formulation of the governing equations. The second is that the so-called separation of rigid body displacements becomes trivial. Selection of local coordinates along the displaced configuration accomplishes automatically the same effect of removing rigid body displacements.

It has been proved that the finite displacement problem of trusses can be solved not only by the stiffness equation for finite displacement, but also by that for small displacement, when local coordinate $\boldsymbol{i}_{\bar{1}}$ is selected in the direction parallel to the displaced member axis and when an iterative process converges.

The stiffness matrix of this total Lagrangian formulation becomes equal to the tangential stiffness of the system, when the local coordinate $\boldsymbol{i}_{\bar{1}}$ is selected along the displaced member axis. The iterative procedure by the method of successive substitutions is presented to solve the stiffness equation developed in this study and its convergence is discussed. Since the stiffness matrix of this study converges to the tangential stiffness of the system, the simple and most primitive successive substitution procedure becomes equal to the Newton-Raphson iteration, resulting in second order convergence for initial values sufficiently close to a solution.

The stiffness matrix is presented in two different forms. One is the customary form, Eq. (25·a), as the sum of the stiffness matrix for small displacement and geometric matrix. The other is presented in slightly different way by Eq. (25·b). Though the latter form is not reported in any literature, it seems to be preferable by the reason that the quantities irrelevant to the final results are not included in the latter but included in the former as has been discussed before.

It seems essential to perform eigen value analysis for the finite displacement solutions of a complex structure. Path length control is effective to trace the main equilibrium path, however, the detection of bifurcation points is possible only with the help of eigen value analysis. Further, it may be a difficult task to locate a solution on bifurcated paths if information on eigen vectors at the bifurcation points is not available.

A simple two bar truss and a reticulated truss are investigated as numerical examples. In the former, the characteristic of the present formulation and the convergence by the successive substitutions have been demonstrated in detail. The latter example is chosen to show the effectiveness of the present formulation and simple systematic procedure to trace the finite displacement equilibrium paths including the main path and paths after bifurcations.

7. ACKNOWLEDGMENT

The writers are grateful to Dr. Yoshiaki Goto of the Nagoya Institute of Technology for his valuable suggestions and comments during the preparation of this paper. This study is supported in part by the Grant-in-Aid for Scientific Research from the Japanese Ministry of Education, Science and Culture.

REFERENECES

1) Connor, J. J., Logcher, R. D. and Chan, S-C. : Nonlinear analysis of elastic framed structures, Journal of Structural Division, ASCE, Vol. 94, No. ST 6, Proc. Paper 6 011, pp. 1 525~1 547, June 1968.

2) Jagannathan, D. S., Epstein, H. I. and Christiano, P. : Nonlinear analysis of reticulated space trusses, Journal of Structural Division, ASCE, Vol. 101, No. ST 12, Proc. Paper 11 799, pp. 2 641～2 658, December 1975.
3) Rajasekaran, S. and Murray, D. W. : Incremental finite element matrices, Journal of Structural Division, ASCE, Vol. 99, No. ST 12, Proc. Paper 10 226, pp. 2 423～2 438, December 1973.
4) Oliveira, E. R. A. : A method of fictitious forces for the geometrically nonlinear analysis of structues, Computational Methods in Nonlinear Mechanics, The Texas Institute for Computational Mechanics, pp. 383～392, September 1974.
5) Chu, K. H. and Rampetsreiter, R. H. : Large deflection buckling of space frames, Journal of Structural Division, ASCE, Vol. 98, No. ST 12, Proc. Paper 9 455, pp. 2 701～2 722, December 1972.
6) Tezcan, S. S. and Mahapatra, B. C. : Tangent stiffness matrix for space frame members, Journal of Structural Division, ASCE, Vol. 95, No. ST 6, Proc. Paper 6 627, pp. 1 257～1 270, June 1969.
7) Yoshida, Y., Masuda, N. and Matsuda, T. : A discrete element approach to elastic-plastic large displacement analysis of thin shell structures, Proc. of Japan Society of Civil Engineers, No. 288, pp. 41～55, August 1979, (in Japanese).
8) Austin, W. J. and Ross, J. J. : Elastic buckling of arches under symmetrical loading, Journal pf Structural Division, ASCE, Vol. 102, No. ST 5, Proc. Paper 12 149, pp. 1 085～1095, May 1976.
9) Iwakuma, T. and Nishino, F. : A consideration on numerical analysis of finite displacement problems, Proc. of 33 th Annual Conference of Japan Society of Civil Engineers, I －19, pp. 55～56, September 1978, (in Japanese).
10) Hangai, Y. and Kawamata, S. : Nonlinear analysis of space frames and snap-through buckling of reticulated shell structures, International Association for Shell Structures, Pacific Symposium Part II on Tension Structures and Space Frames, Tokyo and Kyoto, Japan, Oct. 1971.
11) Hirata, T. and Shirasawa, K. : Nonlinear analysis of a circular arch by the finite element method, Proc. of Matrix Analysis Symposium, 7 th Convention of the Society of Steel Construction of Japan, pp. 341～349, June 1973, (in Japanese).
12) Thompson, J. M. T. and Hunt, G. W. : A General Theory of Elastic Stability, John Wiley and Sons, London, 1973.
13) Galagher, R. H. : Perturbation procedures in nonlinear finite element structural analysis, Computational Methods in Nonlinear Mechanics, The Texas Institute for Computational Mechanics, pp. 9, September 1974.
14) Hosono, T. : Analysis of elastic bucking problem by arc length method, Part 1. The nature of incremental solution at the bucking point, Transactions of the Architectural Institute of Japan, AIJ, No. 242, pp. 41～48, April 1976, (in Japanese).
15) Hosono, T. : Analysis of elastic buckling problem by arc length method, Part 2. The arc length method for actual numerical analysis, Transactions of the Architectural Institute of Japan, AIJ, No. 243, pp. 21～30, May 1976, (in Japanese).
16) Ai, M. and Nishino, F. : A theoretical formulation of thin-walled beam elements within small strains under finite displacements, Proc. of Japan Society of Civil Engineers No. 318, pp. 7～20, February 1982, (in Japanese).
17) Hilderbrand, F. B. : Numerical Analysis, Second Edition, McGraw-Hill Book Company, New York, 1974.
18) Hildebrand, F. B. : Methods of Applied Mathematics, Second Edition, Prentice Hall, Inc., New Jersey, 1965.
19) Yoshida, Y., Masuda, N., Morimoto, T. and Hirosawa, N. : An incremental formulation for computer analysis of space framed structures, Proc. of Japan Society of civil Engineers, No. 300, pp. 21～31, August 1980, (in Japanese).

(Recieved March 26, 1982)